Published in final edited form as:
J Neuropathol Exp Neurol. 2012 April ; 71(4): 348–359. doi:10.1097/NEN.0b013e31824ea078.

Moderate Traumatic Brain Injury Triggers Rapid Necrotic Death of Immature Neurons in the Hippocampus

Hongzhen Zhou, PhD[1,6], **Liang Chen, PhD**[2,3,4,6], **Xiang Gao, PhD**[2,3,4], **Bingde Luo, PhD**[5], and **Jinhui Chen, PhD**[2,3,4]

[1]Nafang Hospital, Southern Medical University, Guangzhou, China

[2]Spinal Cord and Brain Injury Research Group, Indiana University, Indianapolis, Indiana

[3]Stark Neuroscience Research Institute, Indiana University, Indianapolis, Indiana

[4]Department of Neurosurgery, Indiana University, Indianapolis, Indiana

[5]School of Public Health and Tropical Medicine, Southern Medical University, Guangzhou, China

Abstract

Traumatic brain injury (TBI) causes cell death predominantly in the cerebral cortex but there is additional secondary cell death in the hippocampus. We previously found that the majority of the dying cells in the mouse hippocampus are newborn immature granular neurons in a mouse model of lateral controlled cortical impact (CCI) injury with a moderate level of impact. It is not known how long this selective cell death in the hippocampal dentate gyrus lasts, and how it is induced. Using Fluoro-Jade B and immunohistochemistry, we show that most of the neuron death in the hippocampus occurs within 24 hours post-TBI and that cell death continues at low level for at least another 2 wks in this lateral CCI model. The majority of the dying immature granular neurons did not exhibit morphological characteristics of apoptosis and only a small subpopulation of the dying cells was positive for apoptotic markers. In contrast, most of the dying cells co-expressed the receptor-interacting protein-1, a marker of necrosis, suggesting that immature neurons mainly died of necrosis. These results indicate that moderate TBI mainly triggers rapid necrotic death of immature neurons in the hippocampus in a mouse CCI model.

Keywords

Apoptosis; Cell Death; Hippocampus; Mouse model; Necrosis; Traumatic Brain Injury

INTRODUCTION

Traumatic brain injury (TBI) is a leading cause of death and disability in children and young adults (1, 2). Various experimental TBI models, including controlled cortical impact (CCI) injury (3–7), fluid percussion (8, 9), and stretch injury (10, 11), have shown that TBI induces cell death in the hippocampus. Thus, the hippocampus is one of the most vulnerable brain areas post-TBI in both humans and animals (12). Secondary injury to the hippocampus

Correspondence and reprint requests to: Jinhui Chen, Indiana University, School of Medicine, 980 W. Walnut Street, R3, Indianapolis, IN 46202. Fax: (317) 278-5872; chen204@iupui.edu.

[6]These authors contributed equally.

following TBI correlates with impairment of major cognitive functions and the development of seizures (13).

Hippocampal-associated learning and memory impairment is one of the most significant residual deficits following TBI, and is one of the most frequent patient symptoms (14–16). In part, because of a lack of understanding of the cellular and molecular mechanisms that lead to secondary cell death, there are currently no FDA-approved treatments available to prevent hippocampal cell death post-TBI. Thus, a detailed profile of TBI-induced neuronal injury in the hippocampus, including the time course and mechanism of cell death, and an analysis of the cells that are dying, may suggest potential therapeutic targets and a therapeutic window for treatment.

The distribution and degree of cell death in the hippocampus varies among TBI animal models (17, 18) and with injury severity (6, 19, 20) and age of the animals used (21). For adult mice, we have recently shown that when the CCI model is used and the animals are subjected to a moderate level of injury, the majority of the dying hippocampal cells are largely found in the hippocampal dentate gyrus, where neural stem cells that produce new neurons throughout life reside. The majority of the dying cells in the hippocampal dentate gyrus were found to be newborn immature granular neurons that express the neural cell adhesion molecule (NCAM), but not NeuN, a marker for mature neurons (22). The death of immature neurons can compromise neurogenesis in the hippocampus (22, 23) and contribute to learning and memory impairment following TBI (24).

Excitotoxicity may cause cell death via either apoptosis or necrosis, depending on the intensity of the initiating stimulus and the characteristics of the cell population (25–27). To determine the best time window to facilitate a therapeutic approach that targets immature neuron death in the hippocampus following TBI, we assessed its time course and cell death mechanisms using the apoptotic markers caspase-3 and terminal deoxynucleotidyl transferase dUTP nick end labeling (TUNEL) staining and immunostaining with an antibody against receptor-interacting protein-1 (RIP-1), which has been shown to play critical role in necrotic cell death (28–33).

MATERIALS AND METHODS

Animals

Male C57BL/6 mice (Jackson Laboratories, Bar Harbor, ME) were group-housed and subjected to a 12-hour/12-hour light/dark cycle. Access to food and water was ad libitum. All procedures were performed under protocols approved by Indiana University's Animal Care and Use Committee.

CCI Traumatic Brain Injury

Male mice, 8 to 11 weeks old, were subjected to unilateral moderate lateral CCI injury, as previously described (34–36), with the following exceptions: the depth of deformation was set at 1.0 mm and the piston velocity controlled at 3.0 m/sec. These modifications result in a moderate level of injury using an electromagnetic model (37). Briefly, the mice were anesthetized with Avertin and placed in a stereotaxic frame (Kopf Instruments, Tujunga, CA) prior to TBI. Using sterile procedures, the skin was retracted and a 4-mm craniotomy centered between the lambda and bregma sutures was performed. A point was identified midway between the lambda and bregma sutures and laterally midway between the central suture and the temporalis muscle. The skullcap was carefully removed without disruption of the underlying dura. Prior to the injury, the impacting tip with a diameter of 5 mm was angled perpendicularly to the exposed cortical surface. Sham (non-injured) animals were subjected only to craniotomy, but not CCI injury. The core body temperature of the animals

was maintained at 36–37°C during all surgical procedures and throughout the recovery phase.

Tissue Processing

At 4, 24, 48 and 72 hours and on days 7 and 14 after TBI surgery, the animals (n = 6 per group) were deeply anesthetized with an overdose of Avertin and then perfused transcardially with 0.9% saline, followed by an ice-cold fixative containing 4% paraformaldehyde (PFA) in phosphate-buffered saline (PBS). The brains were removed and fixed overnight in PFA, then cryoprotected for 48 hours in 30% sucrose. Serial coronal sections (30 μm thick) were cut using a cryostat (Microm HM 500 M) and stored at −20°C. The sections were then processed for Fluoro-Jade B (FJB) staining and immunohistochemistry.

FJB Staining

Staining was carried out as previously described (38). Briefly, the sections were incubated for 20 minutes in a solution of 0.06% $KMnO_4$ and then rinsed for 5 minutes in distilled water. They were then incubated for 20 minutes in a 0.0004%-solution of FJB (Histo-Chem, Inc., Jefferson, AR), counterstained for 5 minutes with 4',6-diamidino-2-phenylindole ([DAPI]; Sigma, St. Louis, MO), followed by rinsing in distilled water, and overnight air-drying. The dry slides were mounted with DPX (Fluka-Sigma).

Combined FJB/Immuno Staining Analysis

All sections were rinsed 3 times in PBS and then incubated for 1 hour at room temperature in blocking solution (0.1% Triton X-100, 1% bovine serum albumin [BSA], 5% normal goat serum in PBS), followed by overnight incubation at 4°C with primary antibodies. Sections were then washed 3 times with PBS and incubated for 1 hour at room temperature with secondary antibody. After counterstaining with DAPI for 2 minutes, the sections were washed 3 times with PBS. Finally, they were mounted on slides, rinsed with distilled water (5 minutes) and pretreated with 0.06% $KMnO_4$ (5 minutes). After rinsing with distilled water and incubation in a 0.0004% solution of FJB (5 minutes), they were counterstained with DAPI. Primary antibodies and their final concentrations were as follows: anti-NCAM antibody (1:200, mouse, Millipore, Billerica, MA), anti-NeuN antibody (1:100, mouse, Chemicon, Temecula, CA), anti-activated caspase-3 antibody (1:50, rabbit, Abcam, Cambridge, MA), and anti-RIP antibody (1:200, mouse, BD Transduction Laboratories, Franklin Lakes, NJ). Secondary antibodies (Jackson ImmunoResearch, West Grove, PA) conjugated with cy3 were applied in a dilution of 1:800.

TUNEL Assay

TUNEL assays were performed using a commercial kit (In Situ Cell Death Detection Kit, TMR Red; Roche Diagnostics, Mannheim, Germany). Briefly, tissue sections were fixed for 20 minutes at 25°C with 4% PFA in PBS, pH 7.4, followed by washing with PBS (30 minutes), and incubation (30 minutes on ice, 2–8°C) with permeabilization solution (0.1% Triton X–100, 0.1% sodium citrate, freshly prepared). All sections were then incubated with TUNEL reaction mixture (60 minutes at 37°C, in the dark). Positive control sections were pretreated for 10 minutes with DNase I (10 U/mL in 50 mM Tris-HCl, pH 7.5, with 1 mg/ml BSA; Roche Diagnostics) at 25°C before application of the TUNEL reaction mixture. The sections were then counterstained with DAPI, rinsed with PBS and then mounted on slides.

Microscopy

All sections were analyzed by fluorescence microscopy at 10×–63× primary magnification with an inverted microscopy system (Zeiss Axiovert 200 M) interfaced with a computer-

controlled Zeiss Axio Cam MRc5 digital camera (both from, Carl Zeiss MicroImaging, Inc., Thornwood, NY). Images were captured with Zeiss imaging software (AxioVision, v4.0), and assembled and labeled in Photoshop 7.0 (Adobe Systems, Adobe Systems Inc., San Jose, CA).

Quantification

We first quantified the number of FJB-positive cells in the entire hippocampus and in the different subregions of the hippocampus in each animal in 3 epicenter sections 180 μm apart. The anatomical boundaries of hippocampus and each hippocampal subregion (CA1 and CA3; granular cell layer, [GCL]; molecular layer, [ML], hilus) were identified as described by Amaral and Witter (39). The total number of FJB-positive cells in the entire hippocampus and the numbers of FJB-positive cells in each subregion were determined using a 40× objective. DAPI counterstaining allowed us to exclude cell fragments and cell debris in the counts. The percentages of FJB-positive cells in each subregion were calculated.

We then determined the density of FJB-positive cells in the GCL across the entire hippocampus in 1 of every 6 sections across the entire hippocampal formation (from bregma −0.94 to −3.80 mm). The total number of FJB-positive neurons in the GCL was determined in a double-blinded quantitative histological analysis using a 40× objective. The GCL area (μm^2) was measured using the imaging software and densities of FJB-positive cells in the each GCL were calculated using the cell count divided by section GCL volume. NCAM-positive newborn neurons, NeuN-positive mature neurons, and RIP-1-postive necrotic cells were counted under a fluorescent microscope and percentages of double-positive populations calculated.

Statistical Analysis

All data are presented as mean ± SEM and analyzed using either Student t-test (22, 23) or 1-way ANOVA followed by post hoc comparison of the Dunnett T3 test when the homogeneity of the variances was unequal. The significance level was set at $p < 0.05$.

RESULTS

Spatial distribution of secondary neuronal death in the hippocampus after moderate CCI injury

It has previously been shown that the hippocampus is particularly vulnerable to TBI and that this may contribute to subsequent cognitive impairment (12, 40). Using FJB staining (41, 42), we identified dying neurons in the hippocampal epicenter 24 hours after moderate CCI injury (n = 7); there were dying neurons in the ipsilateral hippocampus (Fig. 1a) and in the neocortex around the lesion (Fig. 1a, inset). The average number of FJB-positive cells in the hippocampus of each epicentral section was 359 ± 21. No FJB-positive cells were seen in the contralateral hippocampus or the cortex (not shown). Higher magnification showed that FJB stained the cell bodies and processes of the dying neurons (Fig. 1b–d). FJB-positive cells were predominantly located in the dentate gyrus (Fig. 1a–d). Because the different regions of the hippocampus are composed of different types of cells that may exhibit varying susceptibilities to traumatic insults (9, 43), we further assessed the distribution of FJB-positive cells in the subregions at 24 hours after TBI. In the GCL, 291 ±19 FJB-positive cells were counted. This represented 80.9% of the dying neurons in the hippocampus overall, whereas there were 0.15 % in CA1, 11.42% in CA3, 5.04% in the hilus, and 1.65% in the molecular layer (ML) (Fig. 1e). Thus, neuronal death in the hippocampus predominantly occurred in the GCL within 24 hours after moderate TBI.

At 3 days after TBI, the total number of FJB-positive cells in the hippocampal epicenter was significantly reduced to 55 ± 3 cells/section. The distribution of FJB-positive cells was: 83.02% in the GCL, 2.37% in CA1, 12.80% in CA3, 0.84% in the hilus, and 0.96% in ML (Fig. 1f). To assess rostral and caudal distribution patterns, we quantified the density of FJB-positive cells in the GCL at the epicenter as well as rostrally and caudally to it. The highest density of dead cells was found in the epicenter; from there, it gradually decreased rostrally and caudally (Fig. 1g).

Temporal profile of neuronal death in the GCL after TBI

Because previous studies suggested that cell death in the hippocampus may last for approximately 2 weeks after TBI (3, 44–46), we assessed neuronal death in the GCL at 4 hours, 24 hours, 2 days, 3 days, 7 days, and 14 days after TBI. At 4 hours there were 32008.5 ±5584.3 cells/mm^3 (n = 6) in the GCL. The number of FJB-positive cells peaked at 24 hours (38131.9 ± 4858.2 cells/mm^3, n = 7), dropped sharply at 48 hours (9150.3 ± 1763.8 cells/mm^3, N = 4, p = 0.008 vs. the 24-hour group), and finally decreased to a very low level after 14 days (3 days, 5840.9 ± 736.1 cells/mm^3, n = 6; 7 days, 5945.0 ± 1509.8 cells/mm^3, n = 6; 14 days, 921.8 ± 666.6 cells/mm^3) (Fig. 2). The average number of dying neurons in each section was less than 2 after 14 days. Thus, neuronal death in the hippocampal dentate gyrus occurs very rapidly following TBI

Immature newborn neurons are persistently vulnerable to TBI

The GCL contains immature and mature granular neurons that might respond differently to an insult at different times post-trauma. Indeed, we previously showed that immature neurons are the cells most vulnerable to TBI and start to die within 4 hours post injury (20). To determine whether immature granular neurons are persistently vulnerable at a later time point, we determined the type of GCL cells that were dying at 4 hours and 7 days after TBI (n = 6 for each group) using a combination of FJB and immunostaining with the cell-type specific markers NCAM for immature neurons and NeuN for mature neurons (47). As expected, NeuN-positive mature granular neurons were located across most of the GCL (Fig. 3a), while NCAM-positive immature granular neurons were found in the inner one-third of the GCL (Fig. 3d). Most FJB-positive cells were located in the inner one-third of the GCL (Fig. 3a, b, d, e), where the majority of the newborn immature granular neurons are located (48). Higher resolution and 3-dimensional reconstruction imaging showed that 40.15% of FJB-positive cells could be co-stained with either NeuN or NCAM antibodies. At later stages the FJB-positive cells could not be stained by either antibody. Among co-labeled cells, only 4.96% colocalized with NeuN (Fig. 3b, c), whereas 35.19% colocalized with NCAM (Fig. 3e, f), which represented 88% of the co-labeled FJB-positive cells. Thus, in agreement with our previous report (22), most of the dying cells in the GCL at 24 hours post-TBI are immature granular neurons (22).

At 7 days after TBI, the number of FJB-positive cells in the GCL was visibly reduced (Fig. 3 g, j). Higher resolution images (Fig. 3h, k) and 3-dimensional reconstruction (Fig. 3i, l) showed that most of the FJB-positive cells did not colocalize with NeuN, but with NCAM-positive cells. Thus, at 7 days after TBI the majority of the dying cells in the GCL are immature granular neurons.

Hippocampal neurons predominantly die of necrosis following moderate TBI

To further characterize the dying immature neurons, we used 2 recognized hallmarks of apoptosis, the cleaved active form of caspase-3 and DNA fragmentation, after sham surgery and at multiple time points post trauma (4 hours, 24 hours, 3 days, and 7 days after TBI; n = 6 in each group). We observed a very small number (258 ± 64/mm^3) caspase-3 positive cells in the GCL of sham-treated mice (Fig. 4a, b). The density of caspase-3-positive cells in the

GCL did not change significantly at 4 hours after injury (326 ± 57/mm^3) (Fig. 4c, d), but was substantially increased 24 hours post injury (2495 ± 312/mm^3, $p < 0.05$ vs. the sham control (Fig. 4e, f). These apoptotic cells represented 6% of the dying FJB-labeled cells. Furthermore, most of the caspase-3-positive cells were located in the outer two-thirds of the GCL, which is mainly composed of mature granular neurons. The density of caspase-3-positve cells returned to a basal level at 3 days (426 ± 82/mm^3 (Fig. 4g, h) and 7 days (304 ± 98/mm^3) (Fig. 4I, j) post-injury. Thus, numbers of caspase-3-positive cells in the GCL increased only slightly and transiently within the first 24 hours after injury. We also observed some caspase-3-positive cells in the neocortex of the same sections (data not shown).

To confirm the above results we used TUNEL staining, a widely used method to detect DNA fragmentation, as another indicator of apoptotic cell death (Figure, Supplemental Digital Content 1, http://links.lww.com/NEN/A322). We observed a transient increase in the number of TUNEL-positive cells in the hippocampal GCL after 24 hours (sham, 126 ± 73/mm^3; 4 hours, 145 ± 75/mm^3; 24 hours, 1433 ± 498/mm^3; 3 days, 170 ± 108/mm^3; 7 days, 189 ± 18/mm^3; $p<0.05$ 24 hours vs. sham control). TUNEL-positive cells were also observed in the cortex (data not shown). Together, these results suggest a small and transient increase of apoptosis in the GCL 24 hours after moderate CCI-TBI. Most of the FJP-positive cells in the GCL exhibited processes with slightly condensed nuclei but no visible fragmentation (Fig. 5), indicating that the immature granular neurons in the GCL predominantly do not undergo apoptosis.

Necrotic cell death is characterized by increased cell volume with organelle swelling and plasma membrane rupture and has been considered to be an uncontrolled form of cell death (49). However, there is increasing evidence that the execution of necrotic cell death may be finely regulated by signal transduction pathways and catabolic mechanisms (50, 51). Because RIP-1 phosphorylation is a marker of necrotic cell death (49), we assessed RIP-1 expression in granule cells 24 hours after injury. We did not observe FJB or RIP-1 in the contralateral hippocampal GCL (Fig. 6a, c, e), but detected abundant FJB-positive granule cells and RIP-1 expression in the ipsilateral dentate gyrus (Fig. 6b, d). The merged image in Figure 6 shows colocalization of FJB-positive cells with the RIP-1 signal. In addition, 3-dimensional reconstruction under high amplification indicated that FJB-positive cells expressed high levels of RIP-1 (Fig. 6 g–j). Quantification revealed that 78.6 ± 5.1% of FJB-positive cells co-expressed RIP-1, suggesting that a high percentage of the cells died of necrosis.

DISCUSSION

Persistent memory dysfunction is associated with hippocampal neuron loss following experimental TBI (24, 52–54). We show that the majority of cell death in the hippocampal GCL peaks at 24 hours and persists up to 14 days after TBI in a lateral CCI mouse model

Previous studies suggest that CCI-TBI causes long-term secondary injuries after the immediate primary impact on the brain (3, 46). Silver staining of degenerating neurons has shown that the area of the brain affected by secondary injury is extensive and long-lasting (3). Although silver staining allows one to outline the areas of neuron degeneration, accurate cell counting and immunostaining of other markers remains difficult (44). The patterns of dying neurons we observed using FJB are quite consistent with those detected using silver techniques. Because at the peak injury time point of 24 hours post-TBI, most dying neurons were in the GCL, the cells in this region appear to be more vulnerable to TBI insult than cells in other subregions in the hippocampus; however, this may reflect the high density of cells in the GCL (55).

The cell death peak within 24 hours post-injury is followed by secondary injury. Interestingly, after the early peak of neuronal degeneration, the density of FJB-positive cells remained at a relatively constant level for several days. This suggests that the therapeutic time window to target neuronal death in the hippocampus would be very narrow, i.e. not later than 24 hours post injury.

The mechanisms of hippocampal neuron vulnerability to TBI are not understood. In rodents and primates, including humans, the hippocampus can support neurogenesis throughout life (56–60). New neurons are continuously generated from neural stem/progenitor cells in the subgranular zone of the dentate gyrus (61, 62). Thus, there are both immature and mature neurons in this area. We previously found that the majority of the dying cells in the hippocampal dentate gyrus in the acute phase post-TBI are 2- to 3-week-old newborn immature granular neurons (22). In the present study we found the ratio of immature to mature degenerating neurons was consistently higher at both acute (4 hours) and subacute (7 days) post-injury time points. This indicates that immature neurons are the major hippocampal neuron population vulnerable to TBI and suggest that immature neurons are potential therapeutic targets.

It is currently not known why immature neurons are so vulnerable to TBI. Recent studies of newborn neurons in the dentate gyrus show that they are electrophysiologically distinct from mature granular neurons in the dentate gyrus (63–68). Newborn immature neurons can be more easily excited than mature neurons due to their unique ion channel expression (69–71). It will be interesting to determine whether newborn neurons display exaggerated excitotoxic responses to neurotransmitters released by the damaged neurons after TBI because of this expression.

Calcium influx-mediated excitotoxicity has been considered a major cause of neuron death when neurons are challenged post-TBI with the excitatory amino acid glutamate (72–74). Excitotoxicity seemingly overlaps with other types of cell death such as apoptosis and necrosis depending on the intensity of the initiating stimulus (75–77). The molecular mechanisms underlying secondary neuronal death in the cortex are complex, overlapping, and temporally variable (78). Triggers of secondary TBI (e.g. glutamate-mediated excitotoxicity) can cause both massive necrosis and apoptosis in the cortex (79). In the present study, FJB staining of degenerating neurons in the hippocampus revealed spindle-shaped cell bodies with clear dendritic processes that did not exhibit the typical nuclear condensation of apoptosis, which suggests that most of them did not undergo apoptotic cell death. Moreover, we assessed cell death by immunostaining with antibodies against caspase-3 or using TUNEL staining and found that at although numbers of caspase-3-positive cells were transiently increased in the hippocampal dentate gyrus over the period of 4 to 24 hours, the density of caspase-3-positive cells was much less than the density of the dying FJB-positive cells in the GCL. Even taking into consideration that caspase-3 and TUNEL staining may only label certain stages of apoptotic cell death cell our data still suggest that only a small portion of the cells in the GCL had apoptotic cell death in this model.

Dying FJB-positive neurons in the GCL co-expressed RIP-1, a marker for a subtype of necrotic cell death. RIP-1 has been shown to play a critical role in necrotic cell death induced by death domain (80–83) and Toll-like receptors (84–86). The upregulated expression of RIP-1 in the hippocampus suggests the presence of necrosis. Moreover, necrostatin-1, an inhibitor that targets RIP-1, has been shown to exert neuroprotective functions and to shield neurons from cell death following CCI-TBI (87). This supports our contention that immature hippocampal neurons mainly die of necrosis and not apoptosis following TBI with a moderate level of impact. When animals are subjected to a higher level

of impact to increase the severity of the injury, the numbers of caspase-3- (88, 89) and TUNEL-positive cells (89–91) in the GCL dramatically increase. Thus, numbers of apoptotic cells in the GCL also vary depending on the severity of the injury.

In conclusion, this study provides a quantitative assessment of the changes occurring in the hippocampus after TBI. In particular, we show that moderate TBI triggers rapid necrotic death of immature neurons in the hippocampus. These results suggest that the development of therapeutic approaches should focus on preventing cell death in the hippocampus, in particular the necrotic death of immature neurons. The optimal window for therapeutic intervention appears to be within 24 hours post-injury.

Supplementary Material

Refer to Web version on PubMed Central for supplementary material.

Acknowledgments

This work was supported through funding from the Indiana Spinal Cord & Brain Injury Research Grants, the Ralph W. and Grace M. Showalter Research Award, Indiana University Biological Research Grant, and NIH grants RR025761 and 1R21NS072631-01A.

REFERENCES

1. McCarthy ML, MacKenzie EJ, Durbin DR, et al. Health-related quality of life during the first year after traumatic brain injury. Arch Pediatr Adolesc Med. 2006; 160:252–260. [PubMed: 16520444]
2. Aitken ME, McCarthy ML, Slomine BS, et al. Family burden after traumatic brain injury in children. Pediatrics. 2009; 123:199–206. [PubMed: 19117883]
3. Hall ED, Sullivan PG, Gibson TR, et al. Spatial and temporal characteristics of neurodegeneration after controlled cortical impact in mice: more than a focal brain injury. J Neurotrauma. 2005; 22:252–265. [PubMed: 15716631]
4. Lighthall JW. Controlled cortical impact: a new experimental brain injury model. J Neurotrauma. 1988; 5:1–15. [PubMed: 3193461]
5. Scheff SW, Baldwin SA, Brown RW, et al. Morris water maze deficits in rats following traumatic brain injury: lateral controlled cortical impact. J Neurotrauma. 1997; 14:615–627. [PubMed: 9337124]
6. Saatman KE, Feeko KJ, Pape RL, et al. Differential behavioral and histopathological responses to graded cortical impact injury in mice. J Neurotrauma. 2006; 23:1241–1253. [PubMed: 16928182]
7. Anderson KJ, Miller KM, Fugaccia I, et al. Regional distribution of fluoro-jade B staining in the hippocampus following traumatic brain injury. Exp Neurol. 2005; 193:125–130. [PubMed: 15817271]
8. Thompson HJ, Lifshitz J, Marklund N, et al. Lateral fluid percussion brain injury: a 15-year review and evaluation. J Neurotrauma. 2005; 22:42–75. [PubMed: 15665602]
9. Lowenstein DH, Thomas MJ, Smith DH, et al. Selective vulnerability of dentate hilar neurons following traumatic brain injury: a potential mechanistic link between head trauma and disorders of the hippocampus. J Neurosci. 1992; 12:4846–4853. [PubMed: 1464770]
10. Morrison B 3rd, Cater HL, Benham CD, et al. An in vitro model of traumatic brain injury utilising two-dimensional stretch of organotypic hippocampal slice cultures. J Neurosci Methods. 2006; 150:192–201. [PubMed: 16098599]
11. Cater HL, Gitterman D, Davis SM, et al. Stretch-induced injury in organotypic hippocampal slice cultures reproduces in vivo post-traumatic neurodegeneration: role of glutamate receptors and voltage-dependent calcium channels. J Neurochem. 2007; 101:434–447. [PubMed: 17250683]
12. Ariza M, Serra-Grabulosa JM, Junque C, et al. Hippocampal head atrophy after traumatic brain injury. Neuropsychologia. 2006; 44:1956–1961. [PubMed: 16352320]

13. Vespa PM, McArthur DL, Xu Y, et al. Nonconvulsive seizures after traumatic brain injury are associated with hippocampal atrophy. Neurology. 2010; 75:792–798. [PubMed: 20805525]
14. Rimel RW, Giordani B, Barth JT, et al. Moderate head injury: completing the clinical spectrum of brain trauma. Neurosurgery. 1982; 11:344–351. [PubMed: 7133350]
15. Thornhill S, Teasdale GM, Murray GD, et al. Disability in young people and adults one year after head injury: prospective cohort study. BMJ. 2000; 320:1631–1635. [PubMed: 10856063]
16. Compagnone C, d'Avella D, Servadei F, et al. Patients with moderate head injury: a prospective multicenter study of 315 patients. Neurosurgery. 2009; 64:690–696. discussion 6-7. [PubMed: 19197220]
17. Morganti-Kossmann MC, Yan E, Bye N. Animal models of traumatic brain injury: is there an optimal model to reproduce human brain injury in the laboratory? Injury. 2010; 41 Suppl 1:S10–S13. [PubMed: 20416875]
18. Statler KD, Jenkins LW, Dixon CE, et al. The simple model versus the super model: translating experimental traumatic brain injury research to the bedside. Journal of neurotrauma. 2001; 18:1195–1206. [PubMed: 11721738]
19. Markgraf CG, Clifton GL, Aguirre M, et al. Injury severity and sensitivity to treatment after controlled cortical impact in rats. J Neurotrauma. 2001; 18:175–186. [PubMed: 11229710]
20. Hellmich HL, Capra B, Eidson K, et al. Dose-dependent neuronal injury after traumatic brain injury. Brain Res. 2005; 1044:144–154. [PubMed: 15885213]
21. Tong W, Igarashi T, Ferriero DM, et al. Traumatic brain injury in the immature mouse brain: characterization of regional vulnerability. Exp Neurol. 2002; 176:105–116. [PubMed: 12093087]
22. Gao X, Deng-Bryant Y, Cho W, et al. Selective death of newborn neurons in hippocampal dentate gyrus following moderate experimental traumatic brain injury. J Neurosci Res. 2008; 86:2258–2270. [PubMed: 18381764]
23. Rola R, Mizumatsu S, Otsuka S, et al. Alterations in hippocampal neurogenesis following traumatic brain injury in mice. Exp Neurol. 2006; 202:189–199. [PubMed: 16876159]
24. Hamm RJ, Dixon CE, Gbadebo DM, et al. Cognitive deficits following traumatic brain injury produced by controlled cortical impact. J Neurotrauma. 1992; 9:11–20. [PubMed: 1619672]
25. Martin L, Al-Abdulla N, Brambrink A, et al. Neurodegeneration in excitotoxicity, global cerebral ischemia, and target deprivation: a perspective on the contributions of apoptosis and necrosis. Brain Res Bull. 1998; 46:281–309. [PubMed: 9671259]
26. Ankarcrona M, Dypbukt J, Bonfoco E, et al. Glutamate-induced neuronal death: a succession of necrosis or apoptosis depending on mitochondrial function. Neuron. 1995; 15:961–973. [PubMed: 7576644]
27. Bonfoco E, Krainc D, Ankarcrona M, et al. Apoptosis and necrosis: two distinct events induced, respectively, by mild and intense insults with N-methyl-D-aspartate or nitric oxide/superoxide in cortical cell cultures. Proc Natl Acad Sci U S A. 1995; 92:7162. [PubMed: 7638161]
28. Degterev A, Hitomi J, Germscheid M, et al. Identification of RIP1 kinase as a specific cellular target of necrostatins. Nat Chem Biol. 2008; 4:313–321. [PubMed: 18408713]
29. Festjens N, Vanden Berghe T, Cornelis S, et al. RIP1, a kinase on the crossroads of a cell's decision to live or die. Cell Death Differ. 2007; 14:400–410. [PubMed: 17301840]
30. Festjens N, Vanden Berghe T, Vandenabeele P. Necrosis, a well-orchestrated form of cell demise: signalling cascades, important mediators and concomitant immune response. Biochim Biophys Acta. 2006; 1757:1371–1387. [PubMed: 16950166]
31. Lee TH, Huang Q, Oikemus S, et al. The death domain kinase RIP1 is essential for tumor necrosis factor alpha signaling to p38 mitogen-activated protein kinase. Mol Cell Biol. 2003; 23:8377–8385. [PubMed: 14585994]
32. Vandenabeele P, Galluzzi L, Vanden Berghe T, et al. Molecular mechanisms of necroptosis: an ordered cellular explosion. Nat Rev Mol Cell Biol. 2010; 11:700–714. [PubMed: 20823910]
33. Vanlangenakker N, Vanden Berghe T, Krysko DV, et al. Molecular mechanisms and pathophysiology of necrotic cell death. Curr Mol Med. 2008; 8:207–220. [PubMed: 18473820]
34. Sullivan PG, Thompson MB, Scheff SW. Cyclosporin A attenuates acute mitochondrial dysfunction following traumatic brain injury. Exp Neurol. 1999; 160:226–234. [PubMed: 10630207]

35. Hall ED, Detloff MR, Johnson K, et al. Peroxynitrite-mediated protein nitration and lipid peroxidation in a mouse model of traumatic brain injury. J Neurotrauma. 2004; 21:9–20. [PubMed: 14987461]
36. Gao X, Enikolopov G, Chen J. Moderate traumatic brain injury promotes proliferation of quiescent neural progenitors in the adult hippocampus. Exp Neurol. 2009; 219:516–523. [PubMed: 19615997]
37. Brody DL, Mac Donald C, Kessens CC, et al. Electromagnetic controlled cortical impact device for precise, graded experimental traumatic brain injury. J Neurotrauma. 2007; 24:657–673. [PubMed: 17439349]
38. Schmued LC, Hopkins KJ. Fluoro-Jade: novel fluorochromes for detecting toxicant-induced neuronal degeneration. Toxicol Pathol. 2000; 28:91–99. [PubMed: 10668994]
39. Amaral DG, Witter MP. The three-dimensional organization of the hippocampal formation: a review of anatomical data. Neuroscience. 1989; 31:571–591. [PubMed: 2687721]
40. Hicks RR, Smith DH, Lowenstein DH, et al. Mild experimental brain injury in the rat induces cognitive deficits associated with regional neuronal loss in the hippocampus. J Neurotrauma. 1993; 10:405–414. [PubMed: 8145264]
41. Schmued LC, Albertson C, Slikker W Jr. Fluoro-Jade: a novel fluorochrome for the sensitive and reliable histochemical localization of neuronal degeneration. Brain Res. 1997; 751:37–46. [PubMed: 9098566]
42. Schmued LC, Hopkins KJ. Fluoro-Jade B: a high affinity fluorescent marker for the localization of neuronal degeneration. Brain Res. 2000; 874:123–130. [PubMed: 10960596]
43. Geddes DM, LaPlaca MC, Cargill RS 2nd. Susceptibility of hippocampal neurons to mechanically induced injury. Exp Neurol. 2003; 184:420–427. [PubMed: 14637111]
44. Hall ED, Bryant YD, Cho W, et al. Evolution of post-traumatic neurodegeneration after controlled cortical impact traumatic brain injury in mice and rats as assessed by the de Olmos silver and fluorojade staining methods. J Neurotrauma. 2008; 25:235–247. [PubMed: 18352837]
45. Fox GB, Fan L, Levasseur RA, et al. Sustained sensory/motor and cognitive deficits with neuronal apoptosis following controlled cortical impact brain injury in the mouse. J Neurotrauma. 1998; 15:599–614. [PubMed: 9726259]
46. Chen S, Pickard JD, Harris NG. Time course of cellular pathology after controlled cortical impact injury. Exp Neurol. 2003; 182:87–102. [PubMed: 12821379]
47. Zhao C, Deng W, Gage FH. Mechanisms and functional implications of adult neurogenesis. Cell. 2008; 132:645–660. [PubMed: 18295581]
48. Altman J, Bayer SA. Mosaic organization of the hippocampal neuroepithelium and the multiple germinal sources of dentate granule cells. J Comp Neurol. 1990; 301:325–342. [PubMed: 2262594]
49. Kroemer G, Galluzzi L, Vandenabeele P, et al. Classification of cell death: recommendations of the Nomenclature Committee on Cell Death 2009. Cell Death Differ. 2009; 16:3–11. [PubMed: 18846107]
50. Golstein P, Kroemer G. A multiplicity of cell death pathways. Symposium on apoptotic and non-apoptotic cell death pathways. EMBO Rep. 2007; 8:829–833. [PubMed: 17721445]
51. Golstein P, Kroemer G. Cell death by necrosis: towards a molecular definition. Trends Biochem Sci. 2007; 32:37–43. [PubMed: 17141506]
52. Thompson HJ, LeBold DG, Marklund N, et al. Cognitive evaluation of traumatically brain-injured rats using serial testing in the Morris water maze. Restor Neurol Neurosci. 2006; 24:109–114. [PubMed: 16720946]
53. Vakil E. The effect of moderate to severe traumatic brain injury (TBI) on different aspects of memory: a selective review. J Clin Exp Neuropsychol. 2005; 27:977–1021. [PubMed: 16207622]
54. Smith DH, Lowenstein DH, Gennarelli TA, et al. Persistent memory dysfunction is associated with bilateral hippocampal damage following experimental brain injury. Neurosci Lett. 1994; 168:151–154. [PubMed: 8028769]
55. Witgen BM, Lifshitz J, Grady MS. Inbred mouse strains as a tool to analyze hippocampal neuronal loss after brain injury: a stereological study. J Neurotrauma. 2006; 23:1320–1329. [PubMed: 16958584]

56. Leuner B, Kozorovitskiy Y, Gross CG, et al. Diminished adult neurogenesis in the marmoset brain precedes old age. Proc Natl Acad Sci U S A. 2007; 104:17169–17173. [PubMed: 17940008]
57. Kuhn HG, Dickinson-Anson H, Gage FH. Neurogenesis in the dentate gyrus of the adult rat: age-related decrease of neuronal progenitor proliferation. J Neurosci. 1996; 16:2027–2033. [PubMed: 8604047]
58. Cameron HA, McKay RD. Adult neurogenesis produces a large pool of new granule cells in the dentate gyrus. J Comp Neurol. 2001; 435:406–417. [PubMed: 11406822]
59. Eriksson PS, Perfilieva E, Bjork-Eriksson T, et al. Neurogenesis in the adult human hippocampus. Nat Med. 1998; 4:1313–1317. [PubMed: 9809557]
60. Kornack DR, Rakic P. Continuation of neurogenesis in the hippocampus of the adult macaque monkey. Proc Natl Acad Sci U S A. 1999; 96:5768–5773. [PubMed: 10318959]
61. Ming GL, Song H. Adult neurogenesis in the mammalian central nervous system. Annu Rev Neurosci. 2005; 28:223–250. [PubMed: 16022595]
62. Kempermann G, Gage FH. Neurogenesis in the adult hippocampus. Novartis Found Symp. 2000; 231:220–235. discussion 35-41, 302-6. [PubMed: 11131541]
63. Lopez de Armentia M, Sah P. Development and subunit composition of synaptic NMDA receptors in the amygdala: NR2B synapses in the adult central amygdala. J Neurosci. 2003; 23:6876–6883. [PubMed: 12890782]
64. Tovar KR, Westbrook GL. The incorporation of NMDA receptors with a distinct subunit composition at nascent hippocampal synapses in vitro. J Neurosci. 1999; 19:4180–4188. [PubMed: 10234045]
65. Ye GL, Yi S, Gamkrelidze G, et al. AMPA and NMDA receptor-mediated currents in developing dentate gyrus granule cells. Brain Res Dev Brain Res. 2005; 155:26–32.
66. Vicini S. GABA comes first to newly generated neurons. Focus on "GABAergic signal to newborn neurons in dentate gyrus". J Neurophysiol. 2005; 94:3661. [PubMed: 16293588]
67. Overstreet Wadiche L, Bromberg DA, Bensen AL, et al. GABAergic signaling to newborn neurons in dentate gyrus. J Neurophysiol. 2005; 94:4528–4532. [PubMed: 16033936]
68. Ge S, Goh EL, Sailor KA, et al. GABA regulates synaptic integration of newly generated neurons in the adult brain. Nature. 2006; 439:589–593. [PubMed: 16341203]
69. Ben-Ari Y. Excitatory actions of gaba during development: the nature of the nurture. Nat Rev Neurosci. 2002; 3:728–739. [PubMed: 12209121]
70. Owens DF, Kriegstein AR. Is there more to GABA than synaptic inhibition? Nat Rev Neurosci. 2002; 3:715–727. [PubMed: 12209120]
71. Sheng M, Cummings J, Roldan LA, et al. Changing subunit composition of heteromeric NMDA receptors during development of rat cortex. Nature. 1994; 368:144–147. [PubMed: 8139656]
72. Saatman KE, Murai H, Bartus RT, et al. Calpain inhibitor AK295 attenuates motor and cognitive deficits following experimental brain injury in the rat. Proc Natl Acad Sci U S. 1996; 93:3428–3433.
73. Palmer AM, Marion DW, Botscheller ML, et al. Traumatic brain injury-induced excitotoxicity assessed in a controlled cortical impact model. J Neurochem. 1993; 61:2015–2024. [PubMed: 7504079]
74. Globus MY, Alonso O, Dietrich WD, et al. Glutamate release and free radical production following brain injury: effects of posttraumatic hypothermia. J Neurochem. 1995; 65:1704–1711. [PubMed: 7561868]
75. Bonfoco E, Krainc D, Ankarcrona M, et al. Apoptosis and necrosis: two distinct events induced, respectively, by mild and intense insults with N-methyl-D-aspartate or nitric oxide/superoxide in cortical cell cultures. Proc Natl Acad Sci U S A. 1995; 92:7162–7166. [PubMed: 7638161]
76. Choi DW. Excitotoxic cell death. J Neurobiol. 1992; 23:1261–1276. [PubMed: 1361523]
77. Martin LJ, Al-Abdulla NA, Brambrink AM, et al. Neurodegeneration in excitotoxicity, global cerebral ischemia, and target deprivation: A perspective on the contributions of apoptosis and necrosis. Brain Res Bull. 1998; 46:281–309. [PubMed: 9671259]
78. Stoica BA, Faden AI. Cell death mechanisms and modulation in traumatic brain injury. Neurotherapeutics. 2010; 7:3–12. [PubMed: 20129492]

79. Raghupathi R, Graham DI, McIntosh TK. Apoptosis after traumatic brain injury. J Neurotrauma. 2000; 17:927–938. [PubMed: 11063058]
80. Chan FK, Shisler J, Bixby JG, et al. A role for tumor necrosis factor receptor-2 and receptor-interacting protein in programmed necrosis and antiviral responses. J Biolog Chem. 2003; 278:51613–51621.
81. Holler N, Zaru R, Micheau O, et al. Fas triggers an alternative, caspase-8-independent cell death pathway using the kinase RIP as effector molecule. Nat Immunol. 2000; 1:489–495. [PubMed: 11101870]
82. Vercammen D, Brouckaert G, Denecker G, et al. Dual signaling of the Fas receptor: initiation of both apoptotic and necrotic cell death pathways. J Exp Med. 1998; 188:919–930. [PubMed: 9730893]
83. Vercammen D, Vandenabeele P, Beyaert R, et al. Tumour necrosis factor-induced necrosis versus anti-Fas-induced apoptosis in L929 cells. Cytokine. 1997; 9:801–808. [PubMed: 9367540]
84. Balachandran S, Roberts PC, Kipperman T, et al. Alpha/beta interferons potentiate virus-induced apoptosis through activation of the FADD/Caspase-8 death signaling pathway. J Virol. 2000; 74:1513–1523. [PubMed: 10627563]
85. Kalai M, Van Loo G, Vanden Berghe T, et al. Tipping the balance between necrosis and apoptosis in human and murine cells treated with interferon and dsRNA. Cell Death Differ. 2002; 9:981–994. [PubMed: 12181749]
86. Ma Y, Temkin V, Liu H, et al. NF-kappaB protects macrophages from lipopolysaccharide-induced cell death: the role of caspase 8 and receptor-interacting protein. J Biolog Chem. 2005; 280:41827–41834.
87. You Z, Savitz SI, Yang J, et al. Necrostatin-1 reduces histopathology and improves functional outcome after controlled cortical impact in mice. J Cereb Blood Flow Metab. 2008; 28:1564–1573. [PubMed: 18493258]
88. Clark RSB, Chen M, Kochanek PM, et al. Detection of single- and double-strand DNA breaks after traumatic brain injury in rats: comparison of in situ labeling techniques using DNA polymerase I, the Klenow fragment of DNA polymerase I, and terminal deoxynucleotidyl transferase. J Neurotrauma. 2001; 18:675–689. [PubMed: 11497094]
89. Kim DH, Ko IG, Kim BK, et al. Treadmill exercise inhibits traumatic brain injury-induced hippocampal apoptosis. Physiol Behav. 2010; 101:660–665. [PubMed: 20888848]
90. Kaya SS, Mahmood A, Li Y, et al. Apoptosis and expression of p53 response proteins and cyclin D1 after cortical impact in rat brain. Brain Res. 1999; 818:23–33. [PubMed: 9914434]
91. Colicos MA, Dash PK. Apoptotic morphology of dentate gyrus granule cells following experimental cortical impact injury in rats: possible role in spatial memory deficits. Brain Res. 1996; 739:120–131. [PubMed: 8955932]

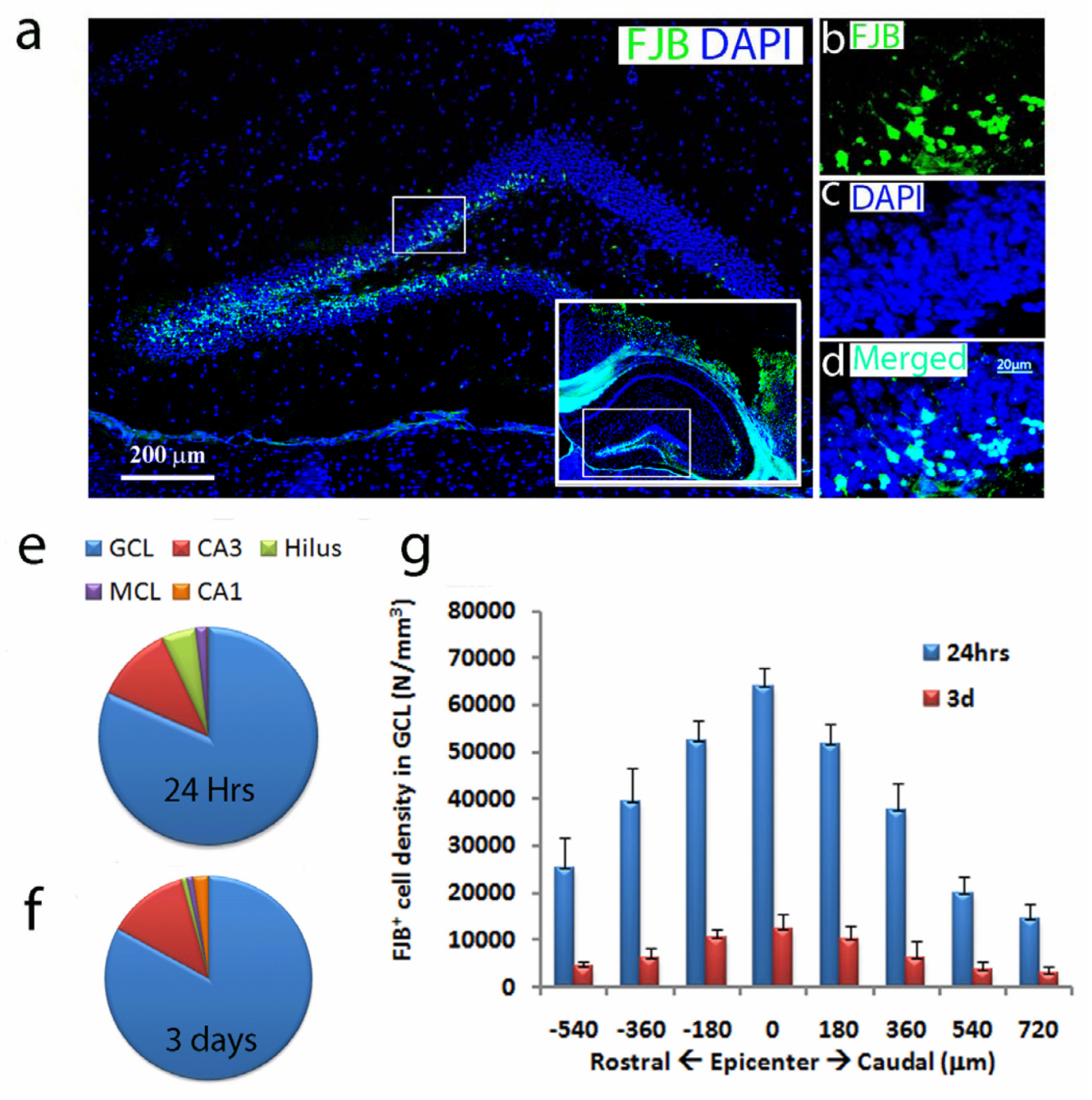

Figure 1.

Distribution of dying neurons in hippocampal subregions after traumatic brain injury (TBI). (**a–d**) Dying neurons 24 hours after TBI are visualized by Fluor-Jade B (FJB) staining (green) in the hippocampus of the ipsilateral hemisphere (**a**). Cell nuclei are counterstained with DAPI (blue). The area indicated by a square is at higher resolution and outlines FJB-positive cells (**b**) and their colocalization with the nuclei in the granular cell layer (**c,d**). (**e, f**) Pie charts demonstrate the average percentage of FJB-positive cells in hippocampal subregions 24 hours (**e**) and 3 days (**f**) after TBI. The column graph illustrates the distribution of FJB-positive cells in the granule cell layer along the rostral-caudal axis at 24

hours (blue bars) and 3 days (red bars) after TBI. GCL, granule cell layer; MCL, molecular layer.

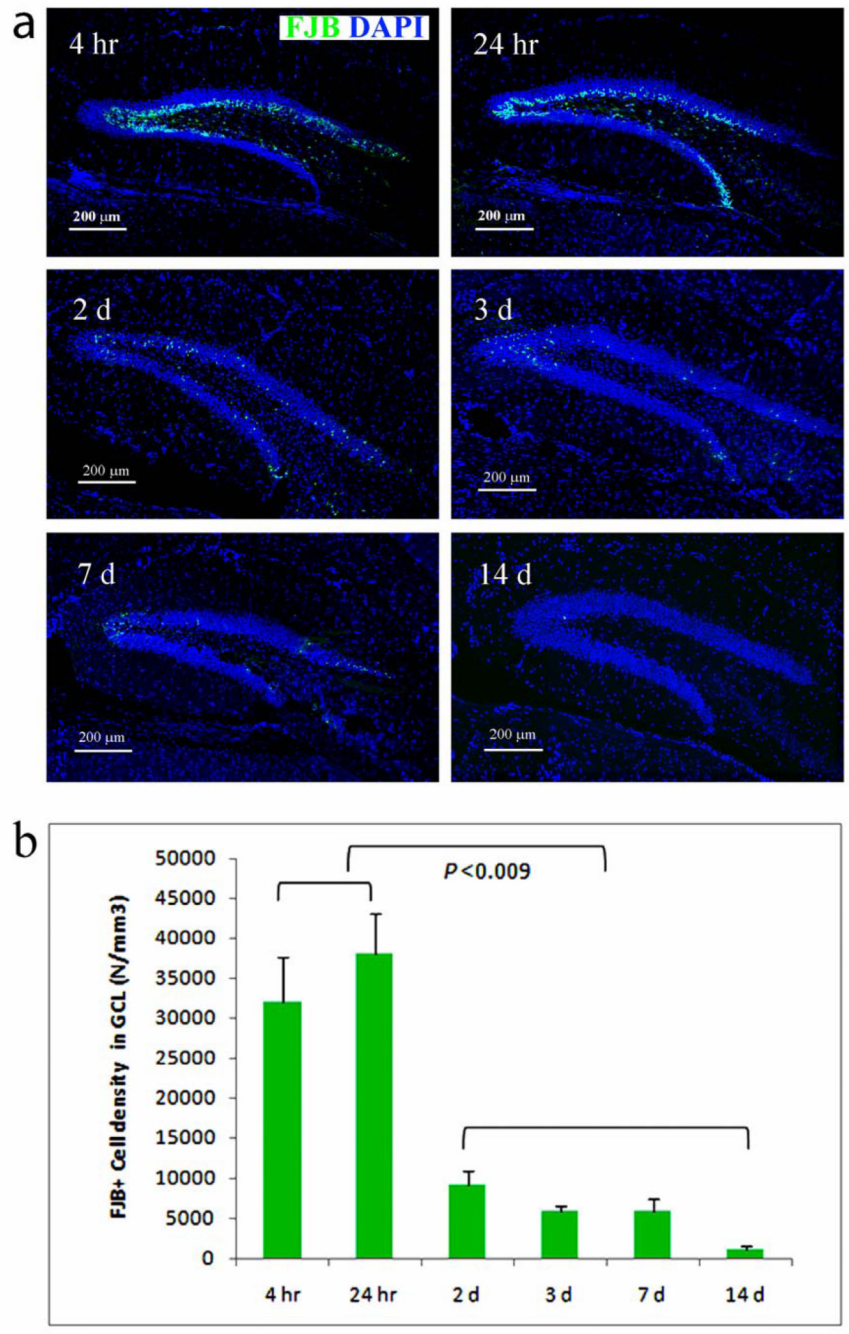

Figure 2.

Temporal dynamics of dying neurons in the granular cell layer (GCL) following traumatic brain injury (TBI). (**a**) Representative images of Fluor-Jade B (FJB)-positive neurons (green) in the granular cell layer at multiple time points (4 hours, 24 hours, 48 hours, 72 hours, 7 days, 14 days) after TBI. Sections were counterstained with DAPI to visualize nuclei in the hippocampal dentate gyrus. (**b**) Graph demonstrates the changes of the density of the FJB-positive cells (N/mm^3) over the time course (4 hours to 14 days). Most of the neurons die within 24 hours after TBI ($p < 0.009$, vs. 24 hours).

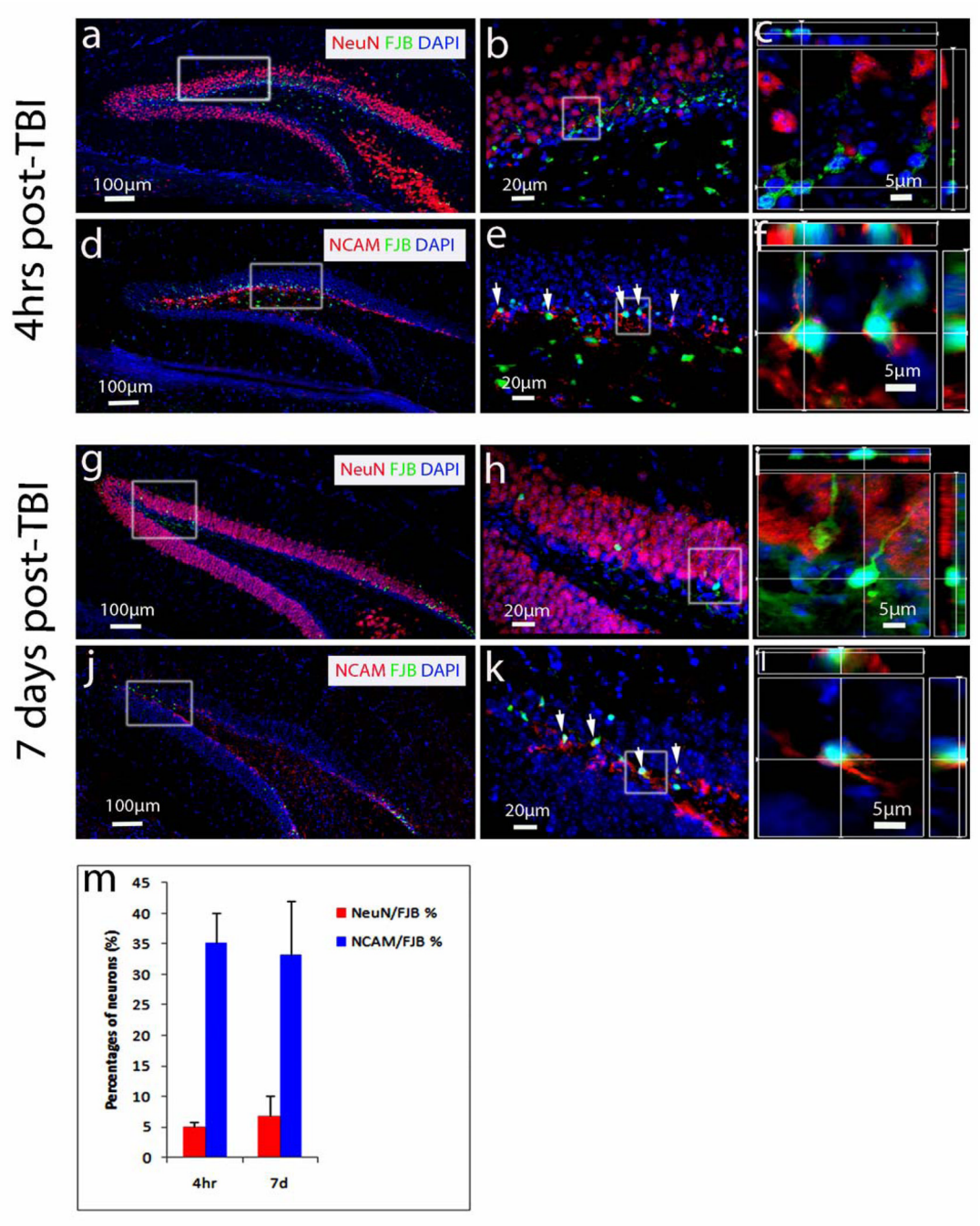

Figure 3.

Colocalization of NeuN- and neural cell adhesion molecule (NCAM)-positive neurons with Fluor-Jade B (FJB)-positive cells. (**a–l**) Representative images of NeuN/FJB (**a–c, g–i**) and NCAM/FJB (**d–f, j–l**) colocalization in hippocampal dentate gyrus 4 hours (**a–f**) and 7 days post-traumatic brain injury (TBI) (**g–l**). The combination of FJB staining (green) with immunostaining using NeuN antibody (red) detects FJB-positive dying cells and mature neurons in the dentate gyrus 4 hours and 7 days after TBI (**a, g**). The combination of FJB staining (green) with immunostaining using NCAM antibody (red) detects FJB-positive dying cells and immature neurons in the dentate gyrus 4 hours and 7 days after TBI (**d, j**). Enlarged images from the white boxes in (**a, d, g, j**) are shown in (**b, e, h, k**) respectively.

Enlarged confocal images from the white boxes in (**b, e, h, k**) are shown with 3-dimensional reconstruction in (**c, f, i, l**), respectively.

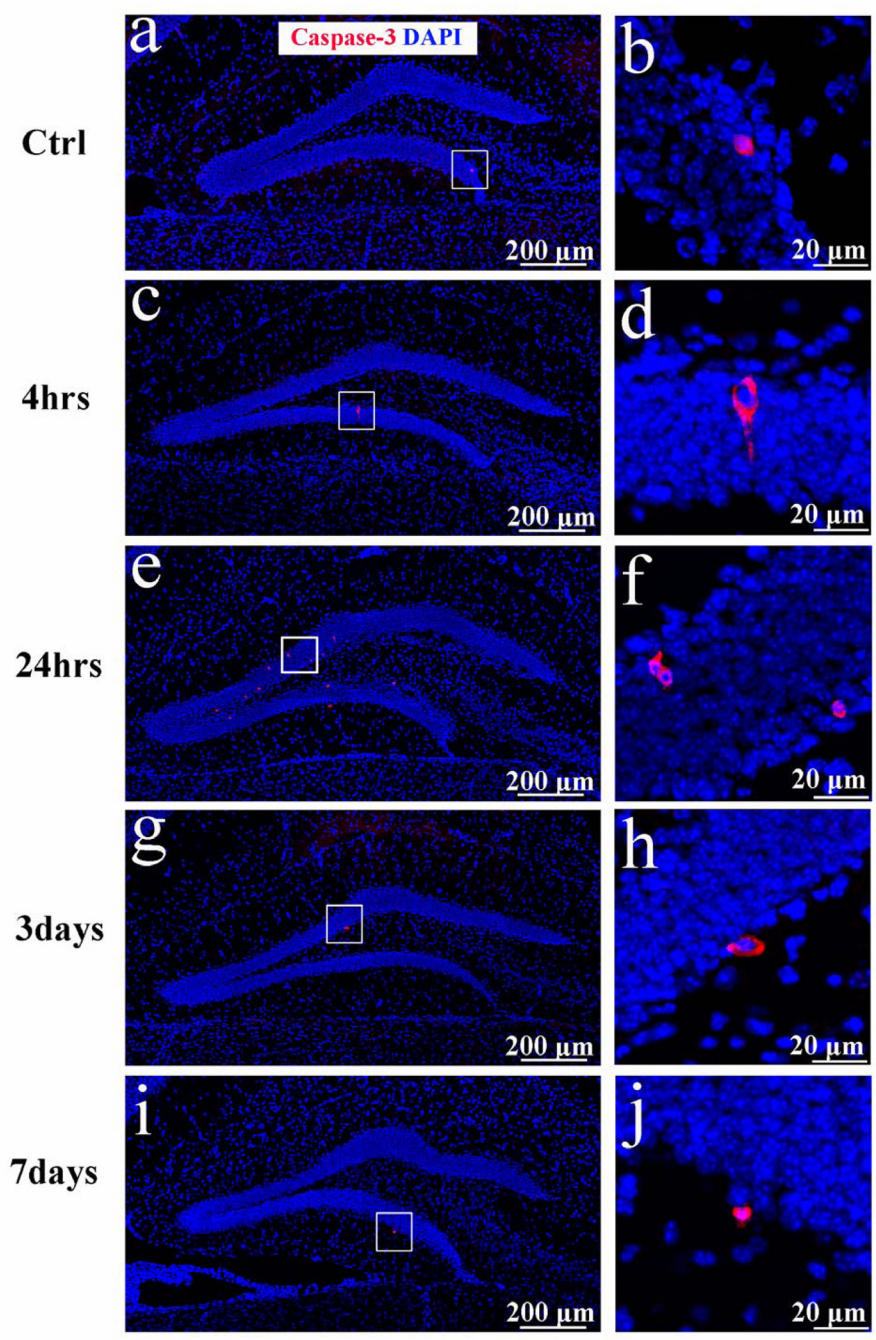

Figure 4.

Caspase-3 immunostaining following traumatic brain injury (TBI). (**a–j**) Caspase-3 immunostaining was performed to examine apoptotic cells in the hippocampal dentate gyrus. Cleaved caspase-3 (red) was detected in the ispilateral side of the sham control (**a, b**) and the injured granular cell layer at 4 hours (**c, d**), 24 hours (**e, f**), 3 days (**g, h**), and 7 days (**i, j**) after TBI. The sections were counterstained with DAPI to visualize the nuclei in the hippocampal dentate gyrus.

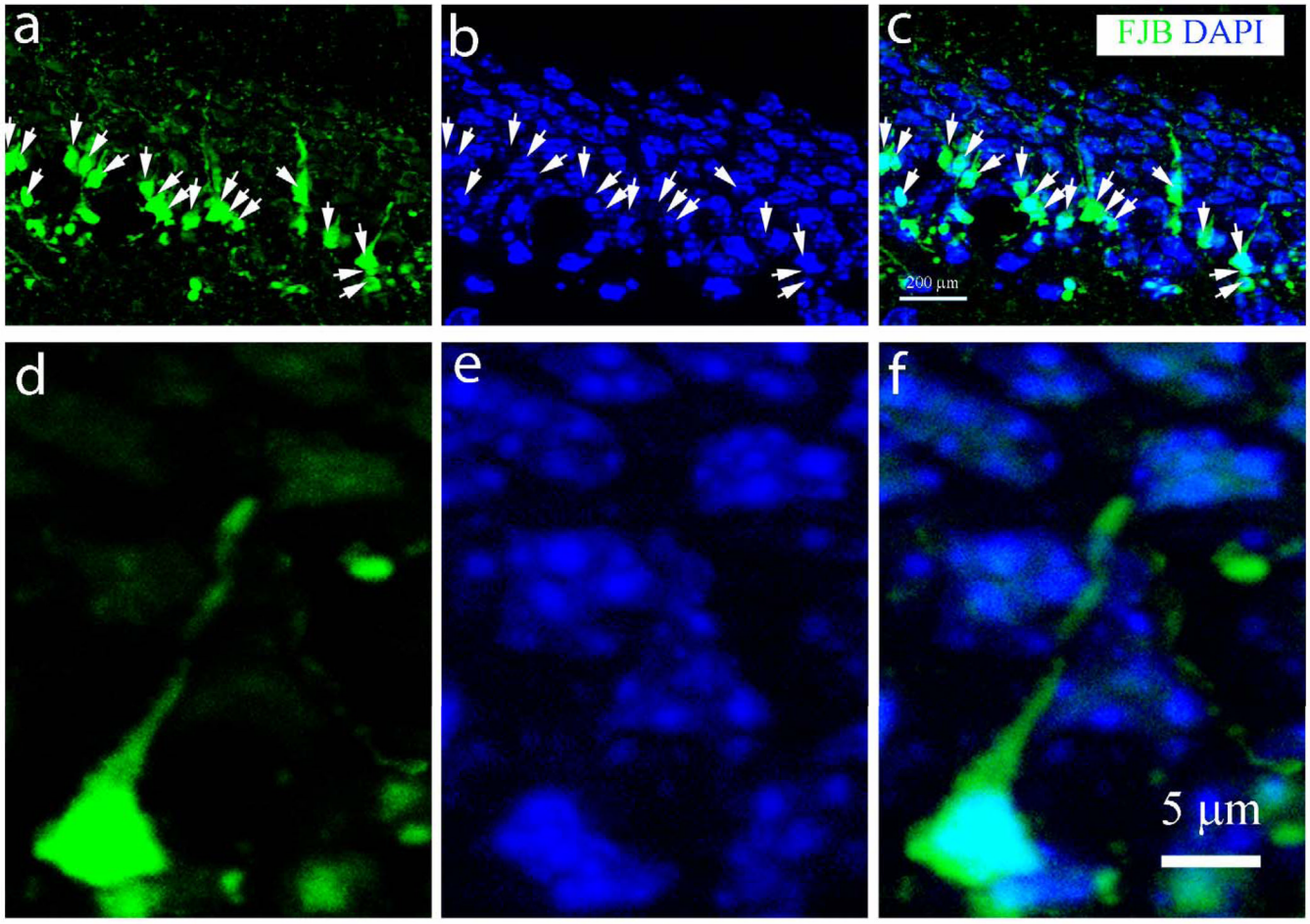

Figure 5.

Morphological analysis of dying neurons in the hippocampal dentate gyrus following traumatic brain injury. (**a–c**) Dying neurons with processes in the inner layer of the granular cell layer (**b**) were stained with Fluor-Jade B (FJB). Arrows in (**a**) and (**c**) indicate green fluorescence. Nuclei counterstained with DAPI identified after image colocalization are indicated by arrows in (**b**). (**d–f**) A single FJB-positive neuron with its process (**d, f**, green) and nucleus (**e**, blue) under higher magnification.

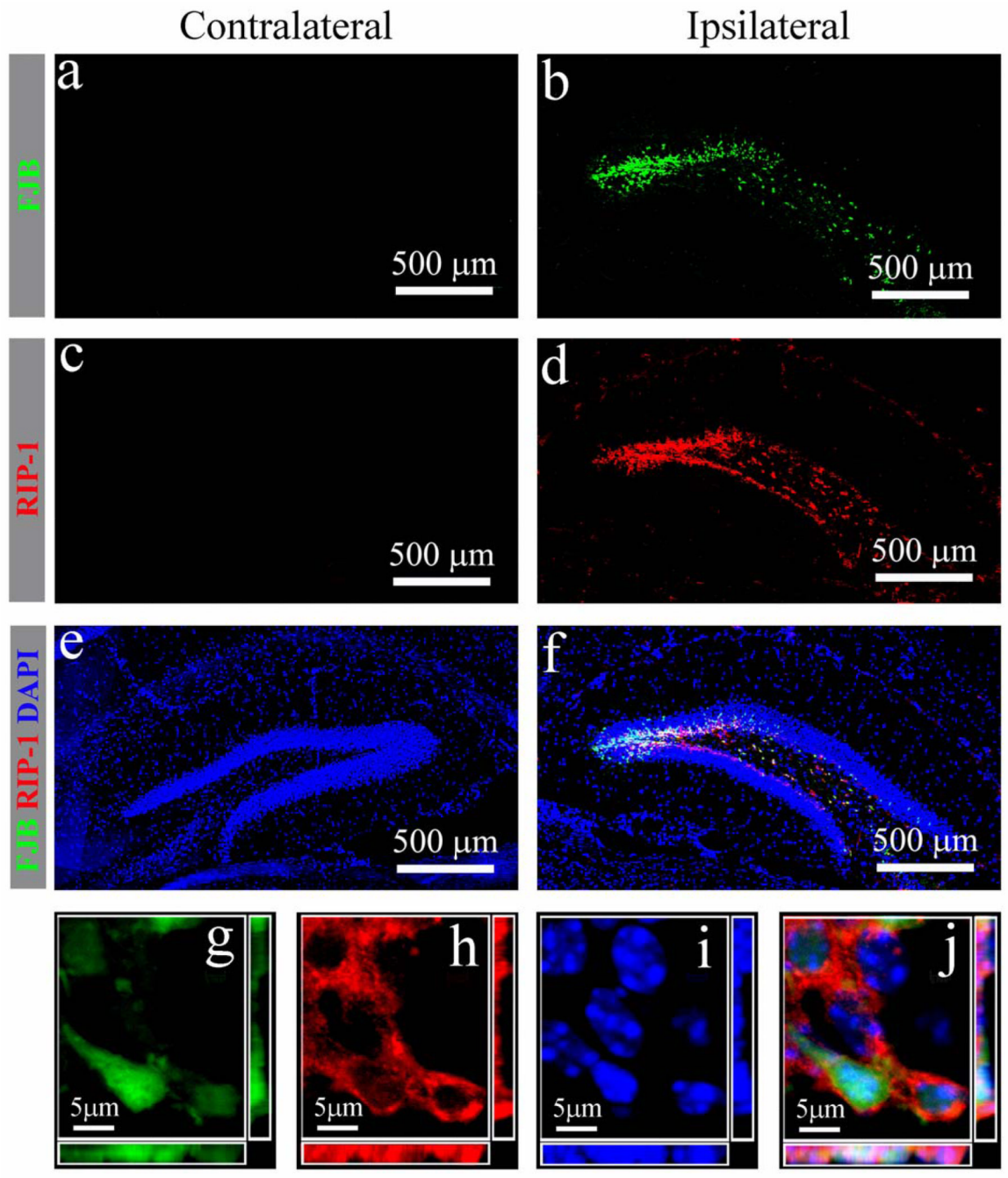

Figure 6.

Receptor interacting protein (RIP-1) expression in injured hippocampal granule neurons after moderate traumatic brain injury. (**a–f**) Distribution of injured neurons (a. b, green) and RIP-1 (**c, d**, red) in the contralateral (**a, c, e**) and ipsilateral (**b, d, f**) hippocampal dentate gyrus 24 hours post injury after combined Fluoro-Jade B (FJB) immunostaining. (**g–j**) A representative 3-dimensional image of the injured granule neurons (**g**) with expression of RIP-1 in the cytoplasm (**h**) and condensed nuclei (**i**) confirms colocalization (**j**) at the single-cell level.